



Experimental investigations on the softening and ratcheting behaviors of steel cylindrical shell under cyclic axial loading

M. Shariati^{a, b *}, H. Hatami^c and M. Damghani Nouri^c

^aMechanical Engineering Faculty, Shahrood University of Technology, Shahrood, Semnan, Iran

^bDepartment of Mechanical Engineering, Faculty of Engineering, Ferdowsi University of Mashhad, Mashhad, Iran

^cMechanical Engineering Faculty, Semnan University, Semnan, Iran

Article Info:

Received: 24/05/2012

Accepted: 16/07/2013

Online: 03/03/2013

Keywords:

Cylindrical shell,
Hysteresis curve,
Cyclic axial loading,
Ratcheting,
Softening.

Abstract

In this research, softening and ratcheting behaviors of Ck20 alloy steel cylindrical shells were studied under displacement-control and force-control cyclic axial loading and the behavior of hysteresis curves of specimens was also investigated. Experimental tests were performed by a servo-hydraulic INSTRON 8802 machine. The mechanical properties of specimens were determined according to ASTM E8 standard. Under force-control loading with non-zero mean force, ratcheting behavior occurred on cylindrical shell and plastic strain accumulation continued up to the collapse point of cylindrical shell. The rate of ratcheting strain became higher using the higher force amplitude. Softening behavior was observed under displacement control loading and, due to the occurred buckling in compression zone, this behavior became more extreme. The behavior of hysteresis curves of this alloy was not symmetrical under tensile and compressive loads. Moreover, the influence of loading history was studied on the behavior of hysteresis curves of the specimens under various types of loadings.

Nomenclature

D	Outer diameter	σ_y	Yield stress
t	Thickness	S_u	Ultimate stress
L	Length	ν	Poisson's ratio
E	Modulus elasticity	Fa	Force amplitude

1. Introduction

Shells have numerous applications in aerospace

industries such as as airplanes and missiles and also in pipelines, marine structures, power plants and nuclear plants.

These shells are under various axial cyclic loadings over their life cycle which decreases their life. Earthquakes are natural loadings which can be applied on these shells [1]. One of the more essential problems which have led to rare investigation of cylindrical shells under

*Corresponding author

Email address: mshariati@shahroodut.ac.ir

cyclic loading is making special fixtures for applying the loads; thus, few studies have been conducted in this field. A study has been done on stainless steel shells, which showed that the displacement amplitude and buckling of shells which are under axial cyclic loadings are less than those of monotonic compressive loadings [2]. Most of the experimental studies on cylindrical shells have been carried out by employing cyclic bending loadings [3-8]. A recent study on cylindrical shells under internal compression has revealed that some parameters including the number of loading cycles, mean stress and stress amplitude are critical factors resulting in the failure of specimens under axial cyclic loadings [9]. Also, another experimental study has been done on cylindrical shells made from magnesium alloys under cyclic loadings. The behavior of hysteresis loops of this specimen has been also analyzed [10-14]. There is another experimental research about shells with square and rectangular cross sections under axial cyclic displacement-control loadings by which the buckling behavior of hysteresis loops are investigated [15]. Another experimental study has been conducted on stainless steel cylindrical shell with the cutout under axial cyclic loading [16]. Experimental tests have been done on the behavior of polyacetal or Polyoxymethylene (POM) under uniaxial cyclic loading. They have demonstrated that the ratcheting strain and strain rate ratcheting are sensitive to the applied stress amplitude and the mean stress [17]. Another study has analyzed buckling behaviors on monotonic and cyclic strain-control loading effects under the influence of different parameters like diameter, length and radius of cylindrical shell [18].

Only buckling behavior under compression loading has been studied on cylindrical shell with cutout. Buckling of composite cylindrical shell with cutout under compression loading and internal pressure has been also investigated [19]. Another study has been done on aluminum cylindrical shells with cutout under compression loading, which studied the effect of size of cutout, position of cutout and aspect

ratio on buckling behavior of specimens [20]. A recent study has been done on the effect of thickness, length and diameter on the buckling behavior of cylindrical shells with elliptical cutout under compression loading [21]. Also, some studies have been performed on the buckling of cylindrical shells with cutout and cracked [22, 23]. Unfortunately, there are just few studies about ratcheting behavior of cylindrical shells under axial cyclic loading conditions, especially those which are made from steel alloys.

In this paper, we analyzed the behavior of hysteresis curves of cylindrical shells under various types of axial cyclic loadings conditions. Moreover, the influences of force amplitude and mean force parameters on cylindrical shells with different lengths made from CK20 alloy steel were investigated. Various types of loadings on specimens were applied step by step and the influence of loading history was studied on the behavior of hysteresis loops.

2. Experimental tests

Experimental tests were carried out by a INSTRON 8802 servo-hydraulic machine. Loads were applied on cylindrical shells in the form of cyclic loadings in both displacement-control and force-control conditions. The number of cycles applying on the specimens ranged from 1 to 1000 cycles depending on the test type. Figure 1 shows the setup of experimental tests. In order to perform cyclic axial loading on cylindrical shells, a fixture was needed which was able to apply tension and compression loading on cylindrical shells without any rotation slip and clearance. Because the specimens were thin, their two sided thread was not possible. So, part no. 2 was used to reinforce two endings of shells. These parts were threaded and each side of them was welded to the cylindrical shell in order to prevent from the separation of shell while loading (Fig. 2). To ensure no deformation in fixtures, a pin was used while adding threaded to the fixture. In Fig. 2, part

no. 1 is a fixture for connection to the device jaw. Part no. 2 was used for cylindrical shell reinforcement in the pin zone. Because of the thin cylindrical shell, it may not be threaded. Therefore, part no. 2 was used for the connection to the fixture. Part no. 3 showed the section of cylindrical shell. Also, in Fig. 1, fixtures can be seen attached to the jaws of the machine and specimen at loading time.

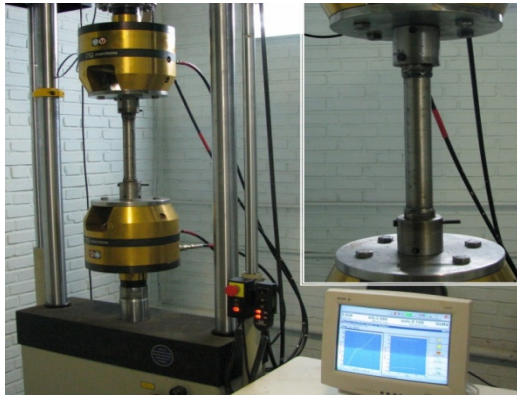


Fig. 1. Cylindrical shell under loading condition by servo-hydraulic machine model INSTRON 8802.

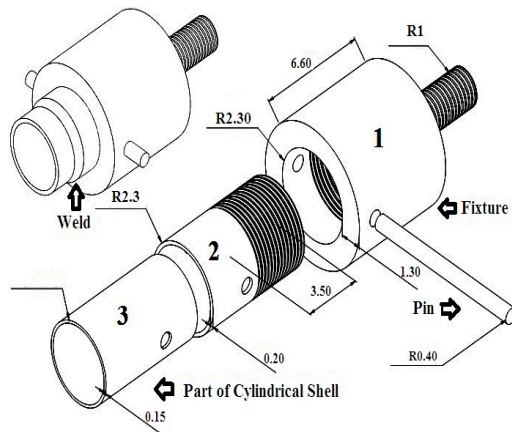


Fig. 2. Schematic layout of typical connections between shell and fixture through welding, thread and use of pin (dimensions are in cm).

2.1. Geometrical and mechanical properties

Cylindrical shells' specimens were made of CK20 alloy steel with the dimensions shown in Table 1. Mechanical properties of this material were obtained according to ASTM E8 standard [24]. Figure 3 shows stress-strain curve of this material.

Table1. Geometrical and mechanical properties of cylindrical shell.

Outer diameter	D=42 mm
Thickness	t=1.5 mm
Length	L=250,300,360,450 mm
Modulus elasticity	E=201 GPa
Yield stress	$\sigma_y = 405$ MPa
Ultimate stress	$S_u = 590$ MPa
Poisson's ratio	$\nu = 0.33$

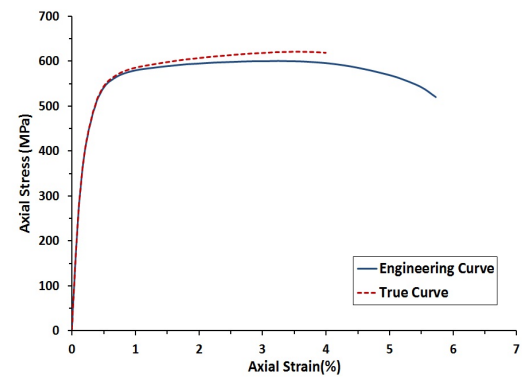


Fig. 3. Stress-strain curve of CK20 steel.

The value of yield stress for this alloy steel was obtained by drawing 0.2% line. As can be seen in this curve, the plastic region of tensile curve was nearly flat.

3. Experimental results and discussion

3.1. Displacement-control tests

3.1.1. Influence of displacement amplitude on the behavior of hysteresis loops

Figure 4 shows the behavior hysteresis loops for three cylindrical shells' specimens with the length equal to 250mm under symmetric displacement-control loading condition. Loadings were applied in three increment steps of displacement amplitude, i.e.: 1.75, 2 and 2.2mm, up to the failure of the specimens. In all three specimens, hardening behavior in tension regions can be observed in few initial cycles. Up to the stabilization of curves and finally failure of shells, softening behavior can be seen

in the same regions. Also, all the specimens showed softening behavior in compression regions. In all the specimens, the residual plastic displacement was higher in compression regions compared with that of tension regions. Hysteresis loops behaved in such a way that inclined to the left hand side of the curve.

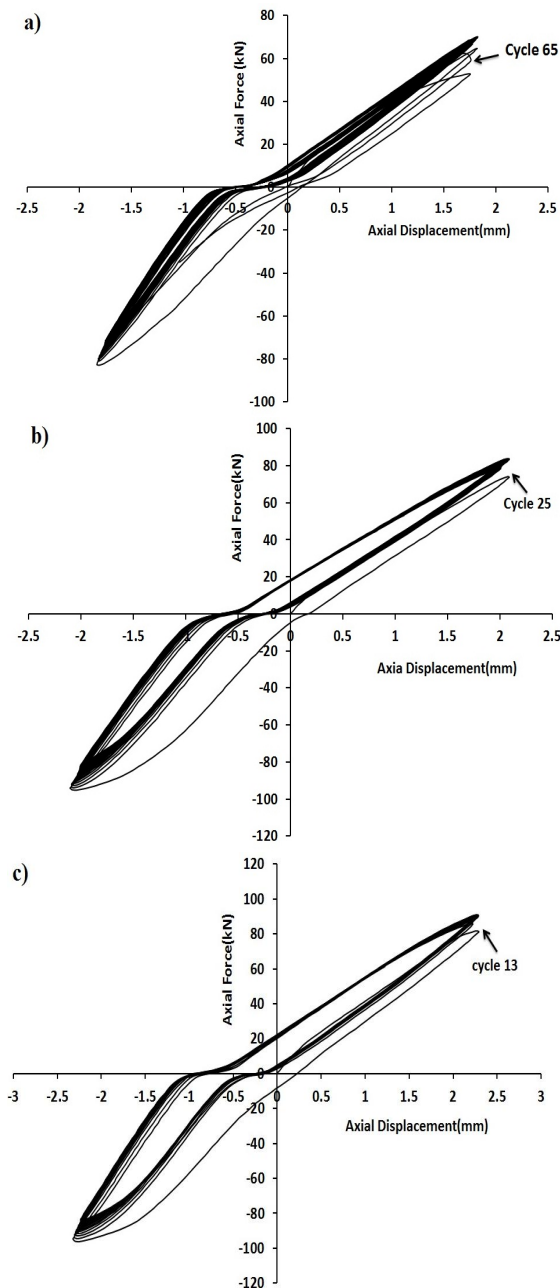


Fig. 4. Hysteresis curves of cylindrical shells with 250 mm length under displacement-control loading with amplitudes: a) 1.75, b) 2 and c) 2.2mm.

Figure 5 shows maximum values of tension and compression forces in each cycle versus the total numbers of cycles up to the failure of the specimens. Accordingly, by increasing displacement amplitude, the slope of softening curve increased in both tension and compression regions. Also, the specimens failed in few initial cycles. In these tests, failure occurred in cycles 65, 25 and 13, corresponding to the order of increasing amplitudes. In tension regions, hysteresis curves showed hardening behavior within few initial cycles and then demonstrated a softening behavior.

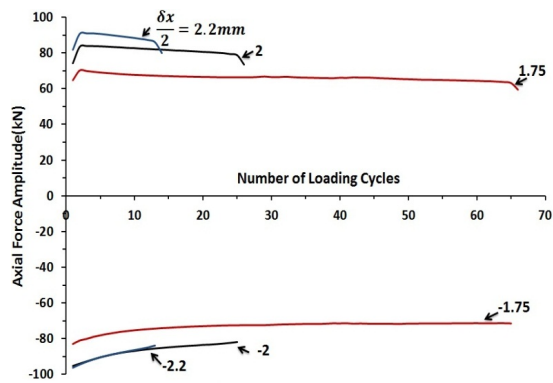


Fig. 5. Variations of force amplitude versus the numbers of cycles for cylindrical shells with 250mm length under displacement-control loading with amplitudes 1.75, 2, 2.2 mm.

Figure 6 shows mean force variations within each hysteresis loop versus the numbers of cycles up to the failure of specimens. Mean force for each hysteresis loop was equal to the average of sum of the maximum tension and compression forces in the same loop. Increasing mean force showed that softening rate in compression regions of hysteresis curves was higher than that of tension regions. In larger displacement amplitudes, the value of mean force increased rapidly and, with the displacement amplitude of 2.2mm, the value of mean force was a positive amount in final cycles. The value of mean force in the first hysteresis loop was more negative for smaller displacement amplitudes. This behavior revealed that endurance capacity of compression sections was higher than that of

the tension sections; however, in larger displacement amplitudes, the mean force of the first hysteresis loop was approaching to zero due to the appearance of local buckling in compression sections of the specimens.

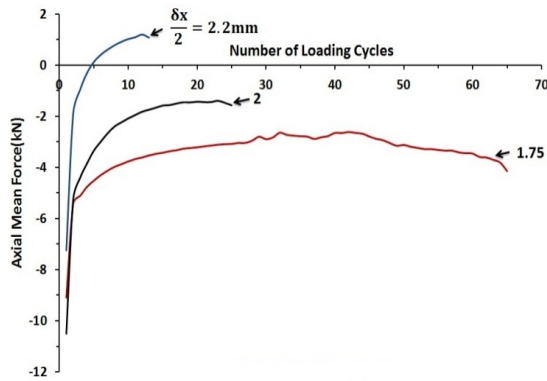


Fig. 6. Variations of mean force versus the numbers of cycles for cylindrical shells with 250mm length under displacement-control loading with amplitudes 1.75, 2 and 2.2mm.

3.1.2. Influence of increasing displacement amplitudes step by step on softening behavior of the specimens

A displacement-control loading was applied on a specimen with 250 mm length step by step as follows: 5 cycles for displacement amplitudes of 0.5 and 0.75 mm and 10 cycles for displacement amplitudes of 1, 1.25, 1.5 and 1.75mm up to the failure of the shell. Figure 7 shows the first hysteresis loops of all displacement amplitudes.

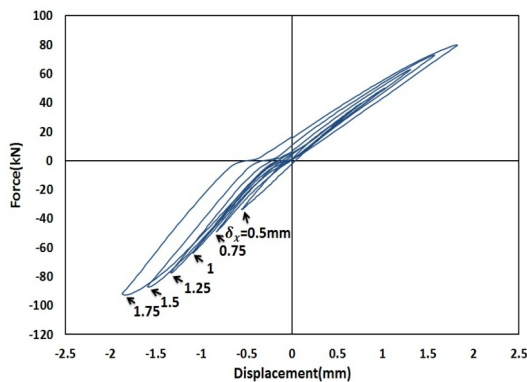


Fig. 7. Hysteresis loops of a specimen with 250mm length and increasing displacement amplitudes from 0.5 to 1.75mm.

Figure 8 shows variations of force amplitudes versus the total numbers of cycles in the same specimen. As can be seen, by increasing displacement amplitude, softening rate in both tension and compression regions increased; however, in larger displacement amplitudes, softening rate was higher in compression region. This behavior was due to the local buckling of compression regions. In larger displacement amplitudes, in few initial cycles, there was a hardening behavior in tension regions; but, after initializing, softening behavior proceeded.

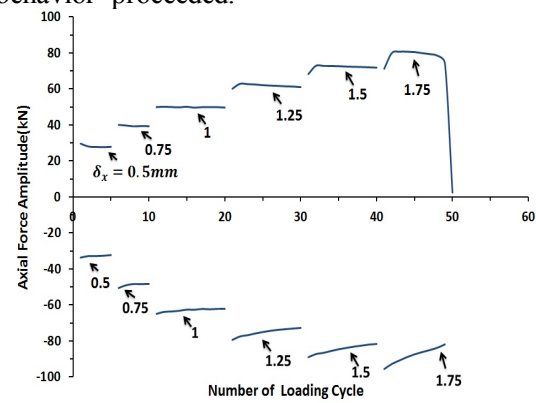


Fig. 8. Variations of force amplitudes versus the numbers of cycles in a specimen with 250mm length and increasing of amplitudes from 0.5mm to 1.75mm.

The comparison of hysteresis curves of amplitude 1.75mm, i.e. Figs. 5 and 8 revealed that the sample, which was under various loading conditions and finally reached the amplitude of 1.75mm, failed in 50 cycles; but, a similar sample with the same length which was only under displacement amplitude of 1.75mm failed in 65 cycles.

3.2. Force-control tests

3.2.1. Influence of force amplitude on the behavior of hysteresis loops

Figure 9 shows hysteresis curves of three cylindrical shells with length of 250mm under symmetric force-control loading with amplitudes of 70, 75 and 80 kN. It is evident that, under constant force, the displacement

amplitude of tension regions was more than that of compression regions, which occurred due to the mechanical properties of materials. Most alloy steels show different behaviors under tensile and compressive loadings. By increasing the force, the increasing displacement amplitude of tension regions would be higher than that of compression regions while accumulation of residual plastic displacement in compression regions is higher than that in tension regions. In these tests, failure occurred in cycles 111, 58 and 18, corresponding to the order of increasing amplitudes.

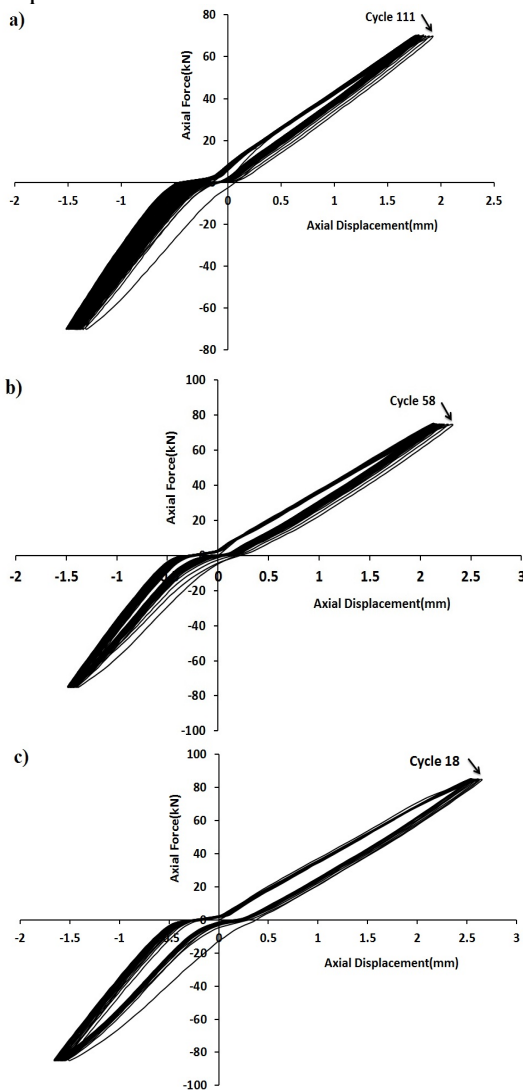


Fig. 9. Hysteresis curves for cylindrical shells with length of 250mm under symmetric force-control loading with amplitudes: a) 70, b) 75 and c) 80 kN.

Figure 10 shows variations of displacement amplitudes versus the numbers of cycles up to the failure of specimens. It is clear that, by increasing force, the displacement amplitudes of compression regions did not increase in accordance with tension regions and, with forces 70 and 75 kN, the displacement amplitudes in compression region were nearly a coincidence. In the force equalling 85kN, the increasing displacement amplitude was higher than the numbers of cycles.

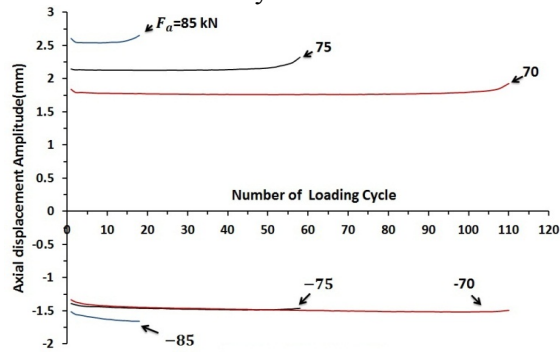


Fig. 10. Variations of displacement amplitudes versus the numbers of cycles for cylindrical shells with length of 250mm under symmetric force-control loading with amplitudes 70, 75 and 80kN.

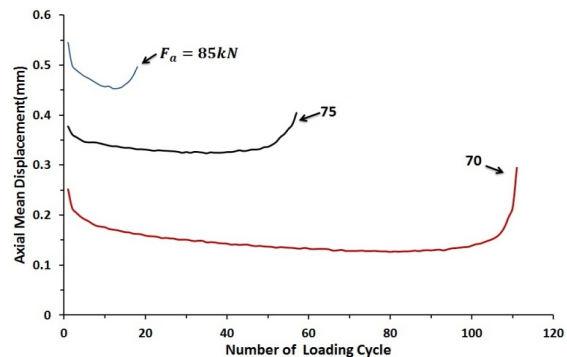


Fig. 11. Variations of center of hysteresis loops versus the numbers of cycles for cylindrical shells with length of 250mm under force-control loading with amplitudes 70, 75 and 80 kN.

It can be concluded from Fig. 10 that, by increasing the numbers of cycles, the increasing rate of displacement amplitude in compression regions was higher than that in tension regions. Also, according to Fig. 11, the displacement of center of hysteresis loops decreased gradually and increased immediately during the failure.

Since displacement amplitudes of tension regions were always higher than those in compression regions, the value of displacement of the center of hysteresis loops was always positive.

3.2.2. Influence of force amplitude and mean force on the ratcheting behavior of cylindrical shells

Figure 12 shows two different tests carried out on cylindrical shells under force-control loading with non-zero mean force. Under this type of loading condition, these specimens showed ratcheting behavior and, during consecutive cycles up to the failure of shells, the accumulation of plastic displacement continued.

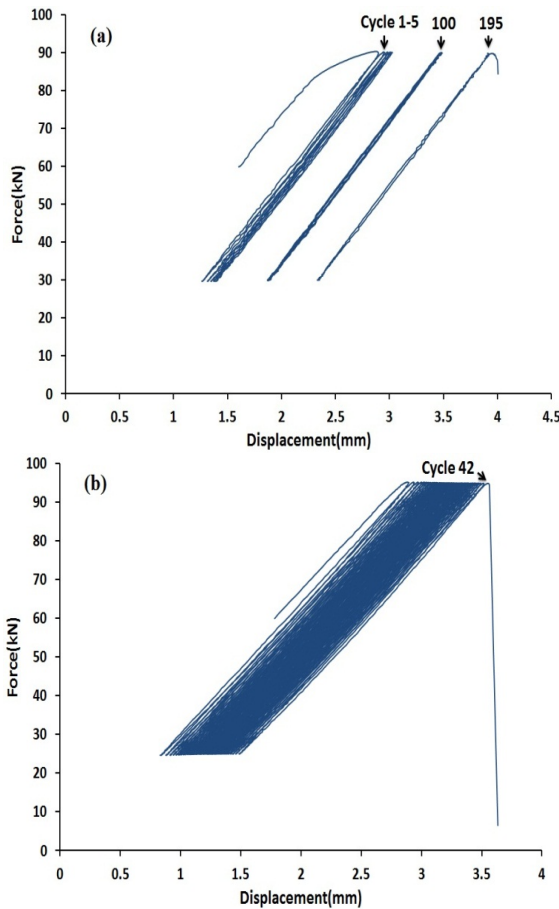


Fig. 12. Ratcheting behavior in cylindrical shells: a) specimen length of 300mm, mean force value of 60kN and force amplitude of 30kN, b) specimen length of 360mm, mean force value of 60kN and force amplitude of 35kN.

Figure 13 shows different specimens under various types of loading conditions with mean force of 60 kN and various force amplitudes. In various lengths, by increasing force amplitude, the slope of ratcheting displacement curve increased and resulted in the failure of shells. Figure 13(a) shows two specimens with length of 300mm under force-control loading with mean force of 60kN and force amplitudes of 25 and 30 kN. Obviously, the specimen which was under force amplitude of 30kN failed in 195th cycle. The same specimen could withstand against failure up to 1000th cycle under force amplitude of 25kN. Furthermore, according to Fig. 13(b), a specimen with length of 360mm under higher values of force amplitudes could withstand against 42 cycles before failure whereas, under force amplitude of 30kN, the same specimen could withstand against failure up to 1000th cycle.

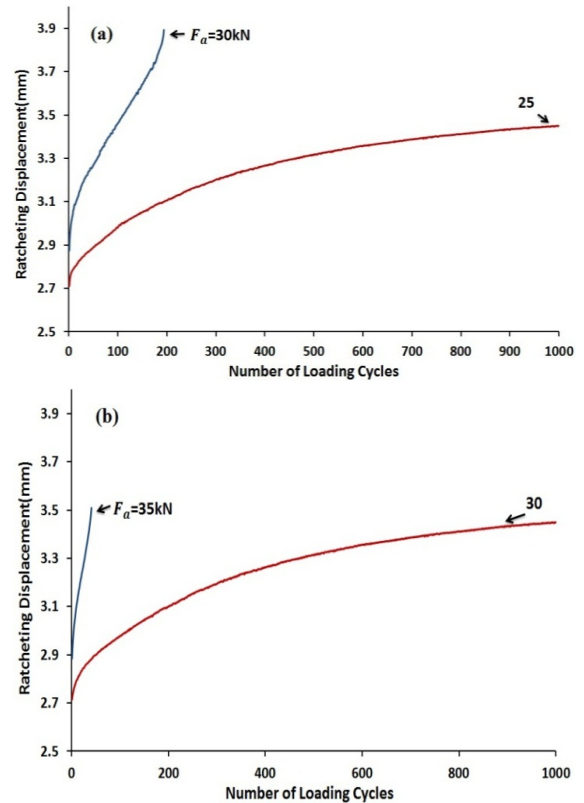


Fig. 13. Comparison of ratcheting behavior of cylindrical shells under mean force of 60kN and various force amplitudes; a) specimen length of 300mm; b) specimen length of 360mm.

3.2.3. Influence of length on the ratcheting behavior of cylindrical shells

By comparing the curves in Fig. 14, it can be understood that, under mean force and similar displacement amplitudes, the slope of ratcheting displacement curve was higher in the specimen with length of 300mm compared with the specimen with length of 360mm, meaning that the shorter specimen would fail sooner. As can be seen in Fig. 14, the specimen with length of 300mm which was under mean force of 60kN and force amplitude of 30kN failed in the 195th cycle whereas the specimen with length of 360mm did not fail up to the 1000th cycle.

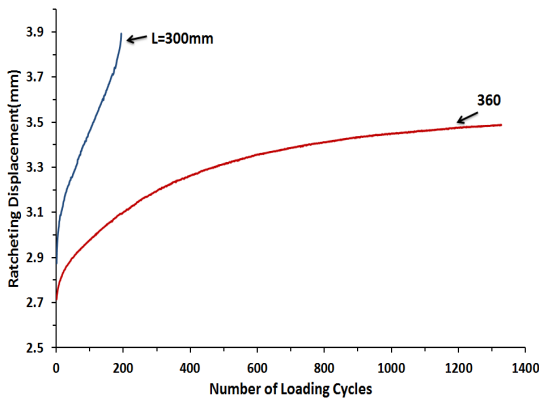


Fig. 14. Comparison of ratcheting behaviors of two cylindrical shells with different lengths under mean force of 60kN and force amplitude of 30kN.

Figure 15 shows ratcheting behaviors of two specimens with lengths of 300mm and 450mm under various force amplitudes. In the 300mm specimen, the force amplitude increased by 10kN after each 10 cycles. Thus, by increasing force amplitude, the specimen showed more ratcheting behavior. The force amplitude in the 450mm specimen increased after each cycle. By comparing Figs. 15(a) and 15(b), it can be seen that, under the same force, increasing displacement amplitude was higher in the shorter specimen.

In Fig. 16, hysteresis curves are compared in the form of tension half-cycle belonging to the 250 mm specimen under force-control loading and increasing of force from 30kN up to 101kN with force amplitudes of 20, 30, 40, 50, 60, 70,

75, 80, 85, 90, 93, 95, 97, 98, 99 and 100kN with monotonic tension curves of specimens with similar lengths under forces 75 and 85kN. In the specimen which was under cyclic tension loading, the value of residual plastic displacement increased by increasing force amplitude. Increasing force was continued by half cycles up to the failure of the specimen. By comparing these two monotonic tensile curves, it can be seen that, with the same force value, displacement of the specimen which was under cyclic loading was higher.

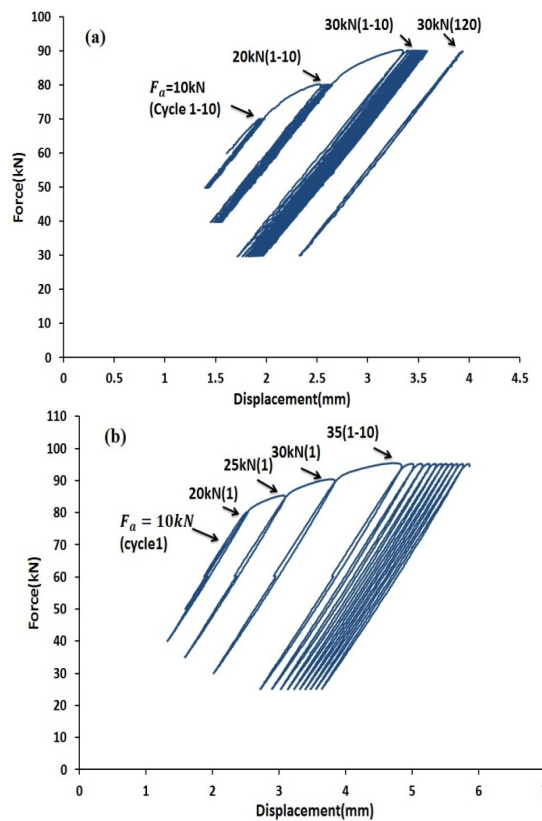


Fig. 15. Ratcheting behavior under force-control loading with mean force equal to 60kN and various force amplitudes; a)300mm specimen length and b)450mm specimen length.

3.2.4. Comparison of tension and compression curves of cylindrical shells under monotonic and cyclic loading

Figure 17 compares hysteresis curves in the form of compression half-cycle belonging to the 250 mm specimen under force-control loading

and increasing of force from -20kN up to -100kN with force amplitudes -20, -30, -40, -50, -60, -70, -75, -80, -85, -90, -95 and -97kN with compression region of the first hysteresis curves of specimens with similar lengths under forces -75 and -85kN, as illustrated in Fig. 9. Increasing compression load was continued until the creation of local buckling, as in Fig. 18(c), near the end side of the specimen. If loading was continued and compression cyclic load was increased, the value of residual plastic displacement would be higher in the compression region of hysteresis loops. Buckling occurred near one of the fixtures. By comparing hysteresis loops of Fig. 17 and two curves of compression region in Fig. 9, in which the force amplitudes were -75 and -85 kN, it was found that compression regions of these two curves under these two types of loadings were generally similar. By increasing compression force, the value of residual plastic displacement would be higher in a cycle compared with its previous cycle. In the last cyclic loading, the specimen buckled with force equal to -75kN whereas the same specimen withstood against -97kN in the previous cycle. This behavior was due to cyclic loadings applied in the form of compression half-cycle on the specimens.

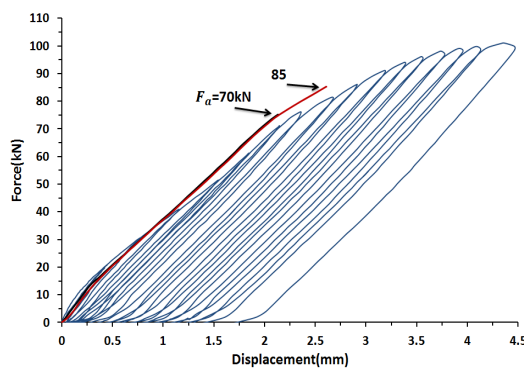


Fig. 16. H curves in the form of tension half-cycle belonging to a 250mm specimen under force-control loading and increasing of tensile force from 20 kN up to 101kN and simple tension curves of cylindrical shells with similar lengths under forces 75 and 85 kN.

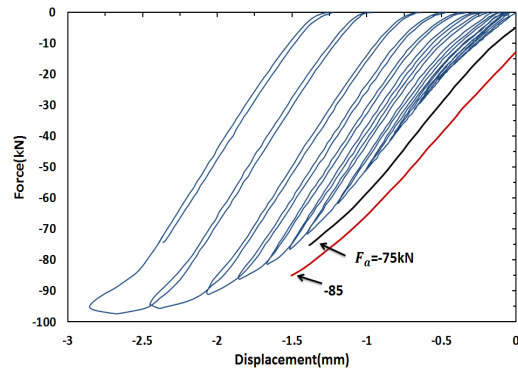


Fig. 17. Hysteresis curves of the 250mm specimen under compression half-cycle loadings and increasing compression force from -20kN until -100kN and comparison of these curves with compression regions of hysteresis curves of cylindrical shells with similar lengths under forces -75 and -85 kN, as illustrated in Fig. 9.

Since welding operation was used to join the cylindrical shells to the fixtures, the ultimate strength of shells was weak near the welded spots; therefore, failure of shells occurred generally in the welded spots [15]. Also, in compressive loadings, shells buckled near the fixtures. At these tests, the failure mode is buckling for the displacement control loading and the failure mode is weld failure for the force control loading. Figure 18 shows a few numbers of specimens which failed near the welded spots and also buckling of shells.

3.3. Influence of loading history

Figure 19 shows two 300mm specimens under mean force of 60kN and different force amplitudes. Figure 19(a) demonstrates a case in which the cylindrical shell was loaded up to 100 cycles with mean force of 60kN and force amplitude of 25kN. Then, this shell was unloaded and again was loaded for another 100 cycles with mean force of 60kN and force amplitude of 30kN. These two loadings were repeated twice on the specimen. Loading condition would be similar but, in the second time, the first loading started with force amplitude of 30kN (Fig. 19(b)). According to Fig. 19(a), the specimen showed a different ratcheting behavior under two loadings with

force amplitude of 25 kN. The reason was the loading applied with force amplitude of 30kN between these two loadings. This 30kN loading generated a work hardening condition



Fig. 18. a) A few numbers of tested cylindrical shells; b) failure of specimen near the welded spots; c) buckling of specimens near the welded fixtures.

in the cylindrical shell. After this 30kN loading, the specimen showed less ratcheting behavior compared with the previous loading. As the specimen was unloaded and again reloaded with force amplitude of 25kN, drop of displacement was sensible after repetition of loading with force amplitude of 30kN. No work hardening phenomena were observed in Fig. 19(b), which was due to this fact that, between two loadings with force amplitude of 30kN, a loading with less force amplitude was applied. After four-

steps of 100 cycles loading, total displacement in Fig. 19(a) was higher than that in Fig. 19(b). This was due to the fact that, in Fig. 19(a), the force amplitude of the first loading was a less value, so only one drop displacement was confronted between loading steps.

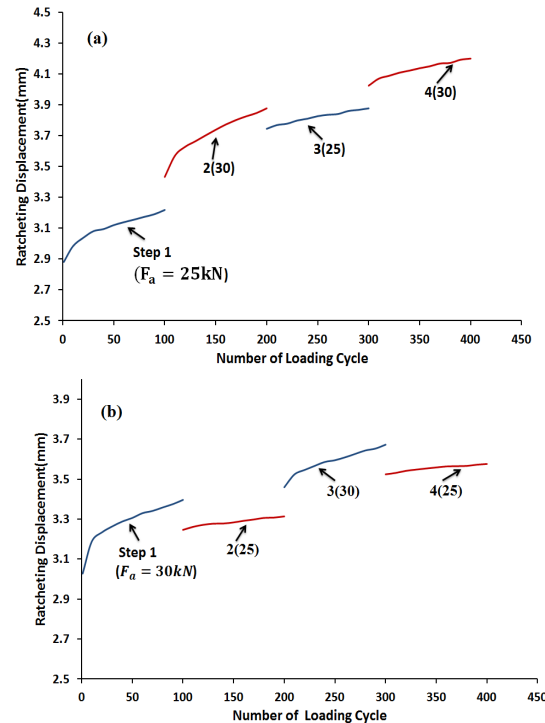


Fig. 19. Loading history of 300mm specimens under mean force of 60 kN and different force amplitudes; a) the order of force amplitudes is 25, 30, 25, 30 kN; b) the order of force amplitudes is 30, 25, 30, 25 kN.

4. Conclusions

According to the experimental test carried out on cylindrical shells under axial cyclic loadings and the comparison of hysteresis loops, the following results were derived:

Under axial symmetric displacement-control loading conditions, increase of displacement amplitude led to increase of softening rate of the specimens. In this case, local buckling occurred in the specimens in the compression region and softening rate in compression region was higher than that in tension region. Also, under this type of loading, the obtained mean force for each hysteresis loop was negative. The

reason was that, in similar displacement amplitudes, the endurance capacity of specimens under compressive forces was higher than tensile forces. This behavior is due to the mechanical properties of CK20 alloy steel.

Under axial symmetric force-control loading conditions, increasing force amplitude increased displacement amplitude rapidly and its value in compression region was higher than that in tension region. But, before buckling the specimens, they failed in tension region. Thus, at first, the displacement amplitude of centers of hysteresis curves decreased and then increased rapidly. Since the displacement amplitude of tension region was higher than compression region during the loading, the displacement amplitude of centers of hysteresis curves was always a positive value.

Under force-control loading conditions and in the presence of non-zero mean force, ratcheting occurred in shells. With similar lengths and mean force, increasing force amplitude increased ratcheting behavior of shells. With similar mean force and force amplitude, decreasing length of shells increased ratcheting behavior and the specimen failed earlier.

Loading history had significant influence on the ratcheting behavior of cylindrical shells so that, if a specific cylindrical shell was subject to the loading up to a given cycle and then this specimen was subject to force amplitude with the value less than that of the first loading, then the ratcheting behavior of this specimen would be less than the case in which the specimen was subject to a loading and no pre-loading was applied on it. This phenomenon was due to work hardening effect, which was created in the cylindrical shell.

If tensile loading was applied on cylindrical shell in the form of half cycle loading, with step by step increase of tensile force and for a given force, the created displacement in this case would be more than that of the simple tensile loading case, which could be due to the accumulation of residual plastic displacements occurring in cyclic loading.

References

- [1] S. C. Kulkarni, Y. M. Desai, T. Kant, G. R. Reddy, P. Prasad, K.K. Vaze and C. Gupta, "Uniaxial and biaxial ratcheting in piping materials—experiments and analysis", *International Journal of Pressure Vessels and Piping*, Vol. 81, pp. 609-617, (2004).
- [2] S. Yoon, S. G. Hong, S. B. Lee and B. S. Kim, "Low cyclic fatigue testing of 429EM stainless steel pipe", *International Journal of Fatigue*, Vol. 8, pp. 1301-1307, (2003).
- [3] M. Elchalakani, X. L. Zhao and R. Grzebieta, "Variable amplitude cyclic pure bending tests to determine fully ductile section slenderness limits for cold-formed CHS", *Engineering Structures*, Vol. 28, pp. 1223-1235, (2006).
- [4] M. Elchalakani, "Plastic mechanism analyses of circular tubular members under cyclic loading", *Thin-Walled Structures*, Vol. 45, pp. 1044-1057, (2007).
- [5] K. H. Chang, W. F. Pan and K. L. Lee, "Mean moment effect of thin-walled tubes under cyclic bending", *Structural Engineering and Mechanics*, Vol. 28, No. 5, pp. 495-514, (2008).
- [6] S. M. Rahman, T. Hassan and E. Corona, "Evaluation of cyclic plasticity models in ratcheting simulation of straight pipes under cyclic bending and steady internal pressure", *International Journal of Plasticity*, Vol. 24, pp. 1756-1791, (2008).
- [7] K. H. Chang and W. F. Pan, "Buckling life estimation of circular tubes under cyclic bending", *International Journal of Solids and Structures*, Vol. 46, pp. 254-270, (2009).
- [8] S. J. Zakavi, M. Zehsaz and M. R. Eslami, "The ratcheting behavior of pressurized plain pipework subjected to cyclic bending moment with the combined hardening model", *Nuclear*

- Engineering and Design*, Vol. 240, pp. 726-737, (2010).
- [9] R. Jiao and S. Kyriakides, "Ratcheting, wrinkling and collapse of tubes under axial cycling", *International Journal of Solids and Structures*, Vol. 46, pp. 2856-2870, (2009).
- [10] S. Begum, D.L. Chen, S. Luo and A. Alan, "Strain-controlled low-cycle fatigue properties of a newly developed extruded magnesium alloy", *The Miners Metals & Materials Society*, Vol. 39, pp. 3014-3026, (2008).
- [11] X. Z. Lin and D. L. Chen, "Strain controlled cyclic deformation behavior of an extruded magnesium alloy", *Materials science and engineering A*, Vol. 496, pp. 106-113, (2008).
- [12] Q. Li, Q. Yu, J. Zhang and Y. Jiang, "Effect of Strain amplitude on tension-compression fatigue behavior of extruded Mg6Al1ZnA magnesium alloy", *Scripta Materialia*, Vol. 62, pp. 778-781, (2010).
- [13] J. Zhang, Q. Yu, Y. Jiang and Q. Li, "An experimental study of cyclic deformation of extruded AZ61A magnesium alloy", *International Journal of Plasticity*, Vol. 27, pp. 768-787, (2010).
- [14] Yu. Qin., J. Zhang, Y. Jiang and Q. Li, "Multiaxial fatigue of extruded AZ61A magnesium alloy", *International Journal of Fatigue*, Vol. 33, pp. 437-447, (2011).
- [15] J. M. Goggins, B. M. Broderick, A. Y. Elghazouli and A. S. Lucas "Experimental cyclic response of cold-formed hollow steel bracing members", *Engineering Structures*, Vol. 27, pp. 977-989, (2005).
- [16] M. Shariati. and H. Hatami, "Experimental study of SS304L cylindrical shell with/without cutout under cyclic axial loading", *Theoretical and Applied Fracture Mechanics*, Vol. 58, pp. 35-43, (2012).
- [17] M. Shariati, H. Hatami, H. Yarahmadi and H. R. Eipakchi, "An experimental study on the ratcheting and fatigue behavior of polyacetal under uniaxial cyclic loading", *Materials & Design*, Vol. 34, pp. 302-312, (2012).
- [18] C. Zhang, Y. Liu, and Y. Goto, "Plastic Buckling of Cylindrical Shells Under Transverse Loading", *Tsinghua Science & Technology*, Vol. 13, pp. 202-210, (2008).
- [19] A. Tafreshi, "Buckling and post-buckling analysis of composite cylindrical shells with cutouts subjected to internal pressure and axial compression loads", *International Journal of Pressure Vessels and Piping*, Vol. 79, No. 5, pp. 351-359, (2002).
- [20] H. Han, J. Cheng, F. Taheri and N. Pegg, "Numerical and experimental investigations of the response of aluminum cylinders with a cutout subject to axial compression", *Thin-Walled Structures*, Vol. 44, pp. 254-270, (2006).
- [21] M. Shariati. and M. M. Rokhi, "Numerical and experimental investigations on buckling of steel cylindrical shells with elliptical cutout subject to axial compression", *Thin-Walled Structures*, Vol. 46, pp. 1251-1261, (2008).
- [22] M. Shariati, M. Sedighi, J. Saemi and H. R. Eipakchi, "Numerical and Experimental Studies on Buckling of Cracked Cylindrical Shells under Combined Loading", *Mechanika*, Vol. 84, pp.12-19, (2010).
- [23] M. Shariati, and M. M. Rokhi, "Buckling of Steel Cylindrical Shells with and Elliptical Cutout", *International Journal of Steel Structures*, Vol. 10, pp.193-205, (2010).
- [24] ASTM E8, Standard Test Methods for Testing of Metallic Materials, *Annual Book of ASTM Standard*, Philadelphia: American Society for Testing and Materials. (1998).